High-temperature structural evolution of caesium and rubidium triiodoplumbates

D.M. Trots, S.V. Myagkota

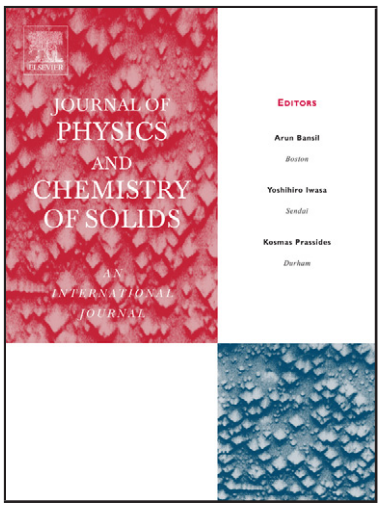

High-temperature structural evolution of caesium and rubidium triiodoplumbates

D.M. Trots, S.V. Myagkota

PII: S0022-3697(08)00173-X
DOI: doi:10.1016/j.jpcs.2008.05.007
Reference: PCS 5491

To appear in: *Journal of Physics and Chemistry of Solids*

Received date: 31 January 2008
Revised date: 2 April 2008
Accepted date: 14 May 2008

Cite this article as: D.M. Trots and S.V. Myagkota, High-temperature structural evolution of caesium and rubidium triiodoplumbates, *Journal of Physics and Chemistry of Solids*, doi:10.1016/j.jpcs.2008.05.007

High-temperature structural evolution of caesium and rubidium triiodoplumbates

D. M. Trots[1,*], S. V. Myagkota[2,3]

[1] HASYLAB at DESY, Notkestraße 85, 22607 Hamburg, Germany

[2] Physics Department, Ivan Franko National University of Lviv, 8 Kyryla i Mefodiya Str., 79005 Lviv, Ukraine

[3] Lviv State Agrarian University, 1 Volodymyra Velykogo Str., 80381 Dublyany-Lviv, Ukraine

Abstract

$CsPbI_3$ and $RbPbI_3$ were investigated by *in situ* powder diffraction within temperature ranges of 298—687 K and 298—714 K, respectively. Both compounds crystallize in orthorhombic *Pnma* symmetry and expand isotropically upon a heating, revealing almost the same relative change of the lattice parameters. A pronounced difference in the structural evolution close to 600 K was observed, namely, $CsPbI_3$ undergoes first order reversible phase transformation $Pnma \xleftrightarrow{563K} Pnma + Pm\bar{3}m \xleftrightarrow{602K} Pm\bar{3}m$, whereas no transitions (except of the sample's melting) in $RbPbI_3$ were detected. An attempt to clarify the relation between the existence/absence of a phase transition and bulging out of the iodine environment around alkaline ions was undertaken.

Keywords: C. X-ray diffraction, D. crystal structure, D. phase transitions, D. thermal expansion

[*] CORRESPONDING AUTHOR. Tel. +49-40-8998-2918, Fax: +49-40-8998-2787, e-mail: d_trots@yahoo.com

Introduction

Optical properties of caesium and rubidium triiodoplumbates have been extensively studied [1, 2] since their implementation as scintillators is of considerable interest [3].

The structure of caesium triiodoplumbate was originally determined by Møller [4]. However, the accuracy of his work was limited by the experimental technique available at that time. The structure of rubidium triiodoplumbate at room temperature was precisely determined by single crystal diffraction [5]: $RbPbI_3$ crystallizes in the orthorhombic symmetry *Pnam* with $a = 10.274(1)$ Å, $b = 17.381(2)$ Å, $c = 4.773(1)$ Å, $Z = 4$ and is isomorphous with $CsPbI_3$. The Pb^{2+} ions are surrounded octahedrally by I^- in this structure. The PbI_6-octahedra are arranged in the double chains along the *c*-axis that are held together by alkaline ions [5]. $CsPbI_3$ and $RbPbI_3$ belong to the structure type of NH_4CdCl_3/Sn_2S_3.

To our knowledge, there are no data on the high-temperature structural evolution of $CsPbI_3$ and $RbPbI_3$ in the literature. The analysis of the results presented in [4] shows that more accurate structural studies of caesium triiodoplumbate are of interest. This requires a more accurate determination of the interatomic distances in the $CsPbI_3$ structure which is the experimental basis for further understanding the correlation between optical and structural properties. Therefore, in the present work we report the results of powder diffraction studies on $CsPbI_3$ and $RbPbI_3$ within temperature ranges of 298—687 K and 298—714 K, respectively.

Experimental

The samples were grown by the Bridgman technique in Lviv [2]. *In situ* diffraction studies at high temperatures were performed at the synchrotron facility Hasylab/DESY (Hamburg, Germany) with the powder diffractometer at beam-line B2 [6]. The 0.3×80

mm quartz capillaries were completely filled with powder samples in air and sealed. Subsequently, the capillaries were mounted in Debye-Scherrer geometry inside a STOE furnace which is equipped with a EUROTHERM temperature controller and a capillary spinner. The furnace temperature was measured by a Pt10%Rh/Pt-thermocouple calibrated using the thermal expansion of NaCl. The wavelength of 0.49328 Å was selected from the direct white synchrotron radiation beam using a Si(111) double flat-crystal monochromator and determined from 8 reflection positions of LaB_6 reference material (NIST SRM 660a). The beam size of 0.4×3 mm at the sample position was cut by the slits. All diffraction patterns have been collected at stabilized temperatures during the heating cycle using an image-plate detector [7] (2θ range 4-45^o). Additional check patterns were taken after the thermal treatment when the samples were cooled down to 298 K. The data evaluation was performed using the "WinPLOTR" [8] software package.

Results

The series of measurements was initially carried out for caesium triiodoplumbate in the 298-770 K temperature range. A change of the sample colour from yellow to dark yellow was observed at the end of thermal treatment during the *in-situ* diffraction study. This can be considered as an evidence for the sample decomposition at high temperatures in air. In order to avoid the sample decomposition, the upper temperature limit was reduced down to 687 K. The additional diffraction check-pattern was collected after the sample was cooled down to 298 K. The colour changes were not revealed for $CsPbI_3$ after its heating up to 687 K, and no difference was observed in the cell volume of $CsPbI_3$ before (892.660(43) Å^3) and after (892.701(49) Å^3) such heat treatment. The Rietveld refinement for $CsPbI_3$ at 298 K was based on the structure

model for a $RbPbI_3$ single crystal [5]. The Rietveld refinement results are presented in figure 1 and the respective values for the structural parameters are summarized in the table 1. The structure is illustrated in figure 2a. The Pb^{2+} ions are located inside the distorted iodine octahedra exhibiting two pairs of equatorial Pb-I distances (3.2259(25) and 3.2775(25) Å) and two apical ones (3.0513(40) and 3.4076(39) Å). The alkaline ion possesses more irregular 9-fold iodine environment, namely, the three pair of iodine at the distances 3.8832(37), 3.8968(35), 3.9312(38) Å and three single iodine atoms at distances 4.0086(47), 4.0271(46), 4.1230(45) Å (figure 2b).

Besides the reflections from the orthorhombic $CsPbI_3$ phase, additional Bragg peaks arise in the diffraction patterns of $CsPbI_3$ at temperatures above 563 K. The phase transition has been found to occur within a temperature range of 563-602 K (figure 3) where the reflections from different structure modifications are present in the $CsPbI_3$ diffraction patterns. The reflections only from the high-temperature modification of $CsPbI_3$ are present in the pattern at 609 K. The analysis of the reflection indices in the high resolution synchrotron diffraction data sets collected above 602 K clearly shows that this new high temperature phase exhibits cubic symmetry (space group $Pm\bar{3}m$, Z=1 and a=6.28940(19) Å at 634 K). Thereafter, the structural parameters of the high-temperature modification of $CsPbI_3$ were refined on the basis of the ideal perovskite structural model (see figure 1 and table 1). In the ideal perovskite structure of the high-temperature modification of $CsPbI_3$, twelve equal Cs–I (4.4473 Å at 634 K) and six Pb–I (3.1447 Å at 634 K) distances are observed. The PbI_6 octahedra are regular, and octahedral axes are parallel to the four-fold $[0\ 0\ 1]_p$ axes of the cubic perovskite cell.

The structure of the high-temperature $CsPbI_3$ modification is illustrated in figure 2c. It reveals a large-amplitude anisotropic thermal vibration of the iodine atoms in the (100) planes. This finding possibly indicates a disorder of iodine in the Cs^+—I^- planes.

In order to achieve the best fit possible we also performed a structure refinement which additionally took the disordered iodine into account. The iodine atoms in 3(d) at (½, ½, ½) sites were distributed along the <100> directions over the 12(h) at (½, *x*, 0) with $x \approx 0.09$ sites in Cs^+—I^- plane. Although the convergence of the refinement was attained for this model, the resulting residuals were R_B=7.5%, R_F=7.2% and χ^2=11.4, compared to R_B =6.43%, R_F =6.28% and χ^2=11.5 for the refinement with single-site I^- ions. Therefore, the preference was given for the model with single-site I^- ions, since it gives a better structural description of $CsPbI_3$ than the disordered model. We suggest that single-crystal measurements of the high-temperature polymorphous modification of $CsPbI_3$ and subsequent structure refinement including anharmonic terms in the structural model would provide more information about the nature of unusual thermal vibrations of iodine. Any 'single-crystal' studies are, however, practically impossible (or at least extremely difficult) even if single crystals are available, since the first order orthorhombic ↔ cubic phase transition in $CsPbI_3$ will lead to fracture (the large volume change of about 6.9% was observed upon this transition). Caesium atoms exhibit large isotropic vibrations in the high-temperature structure of $CsPbI_3$. The similar large amplitudes of isotropic thermal vibrations for the Cs^+ cation and the very unusual thermal vibrations of the halogen ion in the Cs^+—X^- plane were discussed for the cubic perovskite phases of $CsPbCl_3$ and $CsPbBr_3$ [9].

The calculated and experimental diffraction patterns for $RbPbI_3$ are presented in figure 1. The Rietveld refinement was based on the model from reference [5]. The analysis of the structural evolution of $RbPbI_3$ above 298 K does not reveal any phase transition up to 634 K. Further heating up to 714 K leads to the escape of Bragg peaks from the diffraction pattern, *i.e.*, the melting of $RbPbI_3$ sample occurs between 634 and 714 K. The cell volume of 854.261(85) $Å^3$ has been determined at room temperature for

$RbPbI_3$ recrystallized during the *in situ* diffraction experiment. This value agrees with the initial $RbPbI_3$ cell volume of 854.23(12) $Å^3$. The refined structural parameters of $RbPbI_3$ at 298 and 634 K are summarized in table 1. The coordinations of alkaline and Pb^{2+} ions in orthorhombic structures are illustrated in figure 2b. Bond distances and angles of $RbPbI_3$ and both polymorphous of $CsPbI_3$ are presented in table 2.

The temperature dependencies of the $CsPbI_3$ and $RbPbI_3$ cell parameters are presented in figure 3. The values of the lattice parameters increase linearly without any anomalous deviation for both $CsPbI_3$ and $RbPbI_3$ while the temperature changes within 298-687 K range. The relative changes of the cell parameters and volumes in the orthorhombic triiodoplumbates (figure 4) have been calculated in the respective temperature ranges as $\eta x(T) = 100\% \times (x(T) - x(298\ K))/x(298\ K)$, where x corresponds to a, b, c and V parameters. Both $CsPbI_3$ and $RbPbI_3$ samples show the linear isotropic thermal expansion within orthorhombic phases. Furthermore, the volumetric relative expansion is almost the same for caesium and rubidium triiodoplumbates. The volume thermal expansion coefficients were calculated from the temperature dependences of the unit cell volume as $(1/V_0)\times(dV/dT)$, where (dV/dT) is the change of the volume in the corresponding temperature interval and V_0 is the volume at the reference temperature T_0 (T_0 = 298 K in the case of orthorhombic $CsPbI_3$ and $RbPbI_3$ and T_0 = 609 K for cubic $CsPbI_3$). In this way, the volume thermal expansion coefficients of 11.8×10^{-5}, 11.8×10^{-5} and 11.9×10^{-5} K^{-1} have been calculated for orthorhombic $CsPbI_3$, cubic $CsPbI_3$ and orthorhombic $RbPbI_3$, respectively. Temperature dependencies of selected bond distances and volumes of CsI_9, RbI_9, CsI_{12}, PbI_6–polyhedrons in $CsPbI_3$ and $RbPbI_3$ structures are presented in figures 5 and 6, respectively. No anomalous behaviour in those dependences can be observed. Pb−I, Pb−Pb, Cs/Rb−Cs/Rb, Cs/Rb−Pb and I−I distances are very close in both compounds and exhibit quite similar behaviour upon

temperature increase. The main difference in 9-fold iodine environment of alkaline ion is that one of the Rb−I3 distances is 7.4% shorter than the longest one, whereas corresponding Cs−I3 distance in $CsPbI_3$ is only 2.8% shorter. A decrease in the volume of the PbI_6 polyhedron through the orthorhombic↔cubic phase transition is clearly visible in $CsPbI_3$ (figure 6).

Discussion

A minor difference of 0.2% between our (854.23(12) $Å^3$) and the literature (852.33 $Å^3$ [5]) value of the $RbPbI_3$ cell volume at room temperature can be due to the different experimental setups and technique used, whereas the value of 892.71 $Å^3$ [4] for the $CsPbI_3$ cell volume at room temperature agrees well with the 892.66(4) $Å^3$ value resulting from our studies.

Before melting, $CsPbI_3$ undergoes a reversible orthorhombic-to-cubic phase transition *via* a two-phase region ($Pnma \xleftrightarrow{563K} Pnma + Pm\bar{3}m \xleftrightarrow{602K} Pm\bar{3}m$) with a large discontinuous volume change of about 6.9%. This is a very strong indication for the first order phase transition in $CsPbI_3$. In contrast to $CsPbI_3$, no transition into the high-temperature modification was revealed for $RbPbI_3$. An attempt to detect the high-temperature polymorphic modification for rubidium triiodoplumbate has already been made [5] but it was not successful as well. An analysis of available literature data on high-temperature investigations of compounds which are isostructural to $CsPbI_3$ ($TlMnI_3$ and $TlFeI_3$ [10], $InCdBr_3$ [11], $InFeBr_3$ and $InMnBr_3$ [12], $KMnCl_3$ and $TlMnCl_3$ [13], $KMnBr_3$ [14]) has shown the existence of phase transformations in $InFeBr_3$, $KMnCl_3$ and $TlMnCl_3$ in addition to the melting. Crystals of $KMnCl_3$ and $TlMnCl_3$ transform immediately to the perovskite structures upon heating, whereas the reverse phase transitions need comparatively longer period of time [13]. Our experiment

does not show any delay in the reverse phase transition for $CsPbI_3$ (the furnace was cooled to room temperature after heating up to 687 K in about 10 minutes and the pattern from $CsPbI_3$ after temperature treatment was collected in approximately 5 minutes).

The averaged Pb-I distance in PbI_6-octahedra increases from 3.244 Å at 298 K up to 3.266 Å at 593 K for orthorhombic $CsPbI_3$, from 3.144 Å at 609 K up to 3.150 Å at 687 K for cubic $CsPbI_3$ and from 3.231 Å at 298 K up to 3.247 Å at 634 K for orthorhombic $RbPbI_3$. The values for the averaged Pb-I distance are almost the same in both orthorhombic phases and appear to be shorter than the Pb-I distance (3.39 Å) calculated from the sum of the Shannon ionic radii. The last fact may be related to polarizing influence of smaller Pb^{2+} cations on the iodine anion surrounding.

Reference [12] reports the existence of an In^{+}-Br^{-} distance which is about 20% longer than all the other distances in the $InBr_9$-polyhedra of $InFeBr_3$. Similar experimental data are available for $InMnBr_3$ (single elongation of about 20%), $InCdBr_3$ (~16%) and $RbCdBr_3$ (~10%) and they have been explained on the basis of crystal and electronic structure considerations [11]. However, such an elongation is not pronounced for the distances in the 9-fold iodine surroundings of alkaline ions in caesium and rubidium triiodoplumbates. The averaged alkaline-iodine distances increase from 3.958 Å at 298 K up to 4.007 Å at 593 K in $CsPbI_3$ and from 3.872 Å at 298 K up to 3.940 Å at 634 K in $RbPbI_3$. Cs-I distances of the cubic perovskite phase of $CsPbI_3$ vary from 4.446 Å at 609 K up to 4.455 Å at 687 K. Furthermore, the averaged Cs-I distance in $CsPbI_3$ at room temperature is about 0.025 Å shorter than the calculated sum of caesium and iodine Shannon ionic radii (3.98 Å), whereas this is not faithfully for $RbPbI_3$ (averaged Rb-I distance of 3.872 Å is 0.042 Å longer than 3.83 Å value calculated from Shannon ionic radii). Hence, the 9-fold iodine environment of Cs^{+} ion should be more

bulged out in comparison to those of Rb^+; and these conditions may define the existence of a polymorphic phase transition in $CsPbI_3$ or its absence in $RbPbI_3$. In order to check our assumption, the differences between the experimentally determined averaged cation-anion distance and the calculated one using the corresponding Shannon radii were estimated for other compounds of the NH_4CdCl_3 structure type. Similar to caesium triiodoplumbate, the calculated K^+-Br^- distances in $KMnBr_3$, and the Tl^+-I^- distances in $TlMnI_3$ and $TlFeI_3$ appear to be larger than those derived from diffraction studies. However, no high-temperature phase transitions (except the sample melting) were detected for these compounds [10, 14]. We could not find any evidence for relation between an existence/absence of polymorphic phase transitions in $CsPbI_3$/$RbPbI_3$ and the difference in experimentally determined alkali-iodine distances and the ones calculated from the sum of ionic radii.

Conclusions

The structural parameters of improved accuracy were derived for caesium triiodoplumbate by means of synchrotron powder diffraction experiments and the Rietveld refinement technique. $CsPbI_3$ crystallizes in the NH_4CdCl_3-structure, whereas references [15, 16] pointed out distorted perovskite structures for $CsPbCl_3$ and $CsPbBr_3$ (see also references therein [16]). We can therefore confirm the assumption of [17], where a different structure of $CsPbI_3$ was suggested to be responsible for considerable changes of optical properties in the $CsPbX_3$ (X=Cl, Br, I) series.

A pronounced difference in the high-temperature behaviour of the $CsPbI_3$ and $RbPbI_3$ structures was observed: $CsPbI_3$ undergoes a first order reversible phase transition whereas no polymorphic transformations were detected for $RbPbI_3$ before melting. To our knowledge, the conditions that define the presence or absence of a

similar high temperature phase transitions in compounds of the NH_4CdCl_3-structure type are not yet clear. However, further systematic high temperature investigations on $Cs_xRb_{1-x}PbI_3$, $InMn_xFe_{1-x}Br_3$ and $InCd_xFe_{1-x}Br_3$ solid solutions, which are envisaged in the near future, could probably contribute to a better understanding of the relationships between structure parameters and the occurrence/absence of phase transitions in this structure type.

Acknowledgments

The authors are indebt to Dr. G. Stryganyuk (HASYLAB/DESY) and Dr. A. Senyshyn (TU Darmstadt/TU Munich, FRM-II) for the critical manuscript reading as well as to Prof. L. Vasylechko (Lviv Polytechnic National University, Ukraine). We are also grateful to Dr. Th. Vad (TU Dresden) for assisting in the preparation of the manuscript. The HASYLAB/DESY support of Powder Diffractometer at beamline B2 and financial support from the Helmholtz Association of National Research Centres (grant number VH-VI 102) are gratefully acknowledged.

References

[1] A. S. Voloshinovsky, S. V. Myagkota, N. S. Pidzyrailo, Z. A. Khapko, Ukr. Fiz. Zh.+ 32 (1987) 685–687 (in Russian).

[2] S. V. Myagkota, Opt. Spectrosc.+ 87 (1999) 290–294.

[3] S. Zazubovich, Radiat. Meas. 33 (2001) 699–704.

[4] C. K. Møller, Mat. Fys. Medd. Dan. Vid. 32 (1959) 1–18.

[5] H. J. Haupt, F. Huber and H. Preut, Z. anorg. allg. Chem. 408 (1974) 209–213.

[6] M. Knapp, C. Baehtz, H. Ehrenberg, H. Fuess, J. Synchrotron Radiat. 11 (2004) 328–334.

[7] M. Knapp, V. Joco, C. Baehtz, H. Brecht, A. Berghaeuser, H. Ehrenberg, H. von Seggern and H. Fuess, Nucl. Instrum. Meth. A 521 (2004) 565–570.

[8] T. Roisnel, J. Rodriguez-Carvajal, Mater. Sci. Forum 378–381 (2001) 118–123.

[9] J. Hutton, R. J. Nelmes, G. M. Meyer, V. R. Eiriksson, J. Phys. C Solid State 12 (1979) 5393–5410; M. Sakata, T. Nishiwaki, J. Harada, J. Phys. Soc. Jpn. 47 (1979) 232–233.

[10] H.W. Zandbegren, J. Solid State Chem. 37 (1981) 189–203.

[11] R. Dronskowski, J. Solid State Chem. 116 (1995) 45–52.

[12] R. Dronskowski, Inorg. Chem. 33 (1994**)** 5927–5933.

[13] A. Horowitz, M. Amit, J. Makovsky, L. Ben Dor, Z. H. Kalman, J. Solid State Chem. 43 (1982) 107–125.

[14] H.-J. Seifert, E. Dau, Z. anorg. allg. Chem. 391 (1972) 302–312.

[15] Y. Fujii, S. Hoshino, Y. Yamada, G. Shirane, Phys. Rev. B 9 (1974) 4549-4559.

[16] K. Nitsch, V. Hamplova, M. Nikl, K. Polak, M. Rodova, Chem. Phys. Lett. 258 (1996) 518-522.

[17] F. Somma, M. Nikl, K. Nitsch, P. Fabeni, G.P. Pazzi, J. Lumin. 94-95 (2001) 169-172.

Figure captions

Figure 1. The results of Rietveld refinements: points are experimental data, the lines are calculated profiles and the lower curves their differences. Tick marks show the calculated positions of $CsPbI_3$ and $RbPbI_3$ reflections.

Figure 2. The structures of $CsPbI_3$ at room temperature (a) and at T=634 K (c). (b) – iodine surroundings of alkaline and Pb^{2+} cations. Plots (a), (b) and (c) show the thermal ellipsoids at the 100%, 100% and 50% probability level, respectively.

Figure 3. Temperature evolution of cell dimensions of $CsPbI_3$ and $RbPbI_3$. Two dotted vertical lines represent the boundaries of mixed *Pnma* + $Pm\bar{3}m$ region in $CsPbI_3$.

Figure 4. Relative expansions in $CsPbI_3$ and $RbPbI_3$ structures.

Figure 5. Temperature dependencies of selected bound distances in $CsPbI_3$ and $RbPbI_3$ structures. Experimental data points were fitted by second-order polynomials.

Figure 6. Temperature dependencies of volumes of CsI_{12}, CsI_9, PbI_6 and RbI_9 polyhedrons. Data points were fitted by second-order polynomials.

Table 1: Refined structural parameters and R-factors of $CsPbI_3$ and $RbPbI_3$

		$CsPbI_3$		$RbPbI_3$	
Temperature (K)		298	634	298	634
Space group		*Pnma*	$Pm\bar{3}m$	*Pnma*	*Pnma*
a (Å)		10.4581(3)	6.2894(19)	10.2761(9)	10.4200(4)
b (Å)		4.80171(13)	—	4.7793(4)	4.84098(16)
c (Å)		17.7761(5)	—	17.3933(12)	17.6145(5)
V (Å^3) / *Z*		892.66(4) / 4	248.784(13) / 1	854.23(12) / 4	888.53(5) / 4
Cs/Rb	*site*	4(*c*)	1(*b*)	4(*c*)	4(*c*)
	x/a	0.4156(3)	½	0.4166(5)	0.4159(6)
	y/b	¼	½	¼	¼
	z/c	0.82924(19)	½	0.8263(3)	0.8264(4)
	U_{iso} (Å^2)	0.025(3)	0.159(2)	0.033(5)	0.092(9)
	U_{11}	0.024(3)	—	0.044(5)	0.104(9)
	U_{22}	0.032(3)	—	0.034(5)	0.107(10)
	U_{33}	0.017(3)	—	0.020(4)	0.064(8)
	U_{13}	-0.008(2)	—	0.003(3)	0.000(5)
Pb	*site*	4(*c*)	1(*a*)	4(*c*)	4(*c*)
	x/a	0.16049(18)	0	0.1662(2)	0.1662(3)
	y/b	¼	0	¼	¼
	z/c	0.06185(11)	0	0.06001(11)	0.06080(17)
	U_{iso} (Å^2)	0.0111(10)	0.0392(9)	0.0172(16)	0.051(3)
	U_{11}	0.0034(4)	—	0.0237(17)	0.061(3)
	U_{22}	0.0201(15)	—	0.0215(16)	0.046(3)
	U_{33}	0.0097(10)	—	0.0065(14)	0.047(3)
	U_{13}	0.0008(14)	—	-0.0024(15)	-0.009(3)
I1	*site*	4(*c*)	3(*d*)	4(*c*)	4(*c*)
	x/a	0.2997(3)	½	0.3068(3)	0.3048(4)
	y/b	¼	0	¼	¼
	z/c	0.2127(2)	0	0.2149(2)	0.2126(3)
	U_{iso} (Å^2)	0.025(3)	0.194(3)	0.027(3)	0.071(5)
	U_{11}	0.045(3)	0.015(2)	0.039(3)	0.092(5)
	U_{22}	0.015(3)	0.283(3)	0.022(3)	0.069(5)
	U_{33}	0.016(3)	0.283(3)	0.018(3)	0.052(5)
	U_{13}	-0.001(2)	0	-0.011(3)	-0.023(5)
I2 in	*site*	4(*c*)	—	4(*c*)	4(*c*)
4*c*	*x/a*	0.3355(3)	—	0.3396(4)	0.3363(5)
	y/b	¾	—	¾	¾
	z/c	0.99790(19)	—	0.99020(18)	0.9910(2)
	U_{iso} (Å^2)	0.021(3)	—	0.025(3)	0.075(6)
	U_{11}	0.016(2)	—	0.020(3)	0.100(6)
	U_{22}	0.019(3)	—	0.029(3)	0.068(5)
	U_{33}	0.028(3)	—	0.026(3)	0.056(6)
	U_{13}	-0.005(2)	—	0.007(3)	0.002(4)
I3	*site*	4(*c*)	—	4(*c*)	4(*c*)
	x/a	0.0331(3)	—	0.0272(3)	0.0252(4)
	y/b	¼	—	¼	¼
	z/c	0.88541(19)	—	0.8837(2)	0.8860(3)
	U_{iso} (Å^2)	0.015(3)	—	0.018(3)	0.051(5)
	U_{11}	0.013(2)	—	0.015(3)	0.039(5)
	U_{22}	0.022(3)	—	0.035(3)	0.065(5)
	U_{33}	0.009(3)	—	0.003(2)	0.050(5)
	U_{13}	0.001(2)	—	-0.005(2)	-0.006(3)
R_{Bragg}(%) /R_F(%) /χ^2		5.6/6.1/10.1	6.4/6.3/11.5	4.9/5.4/9.3	6.0/9.6/8.2

Table 2: Comparison of bound distances and angles of $CsPbI_3$ and $RbPbI_3$

	$RbPbI_3$ at 298 K	$RbPbI_3$ at 634 K	$CsPbI_3$ at 298 K	$CsPbI_3$ at 634 K	
Cs/Rb - I1 × 2	3.7747(47)	3.8476(59)	3.8892(37)	Cs - I ×12	4.4473
Cs/Rb - I1 × 2	3.8430(48)	3.8928(63)	3.8968(35)	Cs - Pb ×8	5.4468
Cs/Rb – I2 × 2	3.8068(48)	3.8684(62)	3.9312(38)	Cs - Cs ×6	6.2894
Cs/Rb – I3 × 1	3.8164(62)	3.9072(87)	4.0086(47)	Pb - I ×6	3.1447
Cs/Rb – I2 × 1	4.0530(63)	4.1266(80)	4.0271(46)	Pb – Pb×6	6.2894
Cs/Rb – I3 × 1	4.1327(60)	4.2053(76)	4.1230(45)	I - I ×8	4.4473
‹Cs/Rb – I›$_9$	3.872	3.940	3.958	I - I ×6	6.2894
Cs/Rb – Pb × 1	4.8138(56)	4.8815(75)	4.9209(38)		
Cs/Rb – Pb × 2	5.2822(50)	5.3353(68)	5.3842(35)		
Cs/Rb – Pb × 2	5.2873(49)	5.3644(63)	5.4006(33)		
Pb – I1 × 1	3.0568(39)	3.0388(59)	3.0513(40)		
Pb – I2 × 2	3.2162(29)	3.2415(38)	3.2259(25)		
Pb – I3 × 2	3.2576(26)	3.2733(36)	3.2775(25)		
Pb – I3 × 1	3.3822(39)	3.4133(59)	3.4076(39)		
‹Pb – I›$_6$	3.231	3.247	3.244		
Pb – Pb × 2	4.6550(24)	4.7371(38)	4.6763(23)		
I1 – I3 × 2	4.1525(39)	4.2805(59)	4.2717(40)		
I1 – I2 × 2	4.5881(40)	4.6047(54)	4.5259(42)		
I1 – I3 × 2	4.5142(38)	4.5474(53)	4.5738(39)		
I1 – I2 × 1	5.0217(47)	5.1189(64)	5.2632(49)		
I2 – I2 × 2	4.0880(47)	4.1967(60)	4.1962(36)		
I2 – I3 × 1	4.3574(50)	4.3445(66)	4.3775(45)		
I2 – I3 × 2	4.4110(42)	4.4491(55)	4.4457(38)		
I3 – I3 × 2	4.7363(42)	4.7212(64)	4.7792(41)		
I1 – Cs/Rb – I1 × 1	78.538	77.966	76.065		
I1 – Cs/Rb – I1 × 1	76.884	76.894	76.241		
I1 – Cs/Rb – I1 × 2	87.78(10)	87.938(126)	87.714(64)		
I1 – Cs/Rb – I1 × 2	138.445	138.274	136.119		
I1 – Cs/Rb – I2 × 2	71.667(1)	70.442	69.641(1)		
I1 – Cs/Rb – I2 × 2	140.047(1)	140.430	141.320(1)		
I1 – Cs/Rb – I2 × 2	84.337(93)	84.397(125)	86.127(64)		
I1 – Cs/Rb – I2 ×2	134.151	133.599	133.235		
I1 – Cs/Rb – I2 ×2	82.058(77)	82.531(118)	84.598(62)		
I1 – Cs/Rb – I2 ×2	129.96	130.400	131.29		
I1 – Pb – I2 ×2	93.975(3)	92.253	92.234(6)		
I1 – Pb – I3 ×2	91.214(10)	92.103(7)	92.485(5)		
I1 – Pb – I3 ×1	176.754(110)	177.161(166)	174.516(110)		
I2 – Pb – I2 ×1	95.956	96.613	96.189		
I2 – Pb – I3 ×2	84.608(46)	83.651(68)	84.612(42)		
I2 – Pb – I3 ×2	174.727(1)	173.598	175.179(1)		
I2 – Pb – I3 ×2	83.862(2)	83.868(3)	84.115(2)		
I3 – Pb – I3 ×2	90.993(12)	89.807(57)	91.247(10)		

Figure1

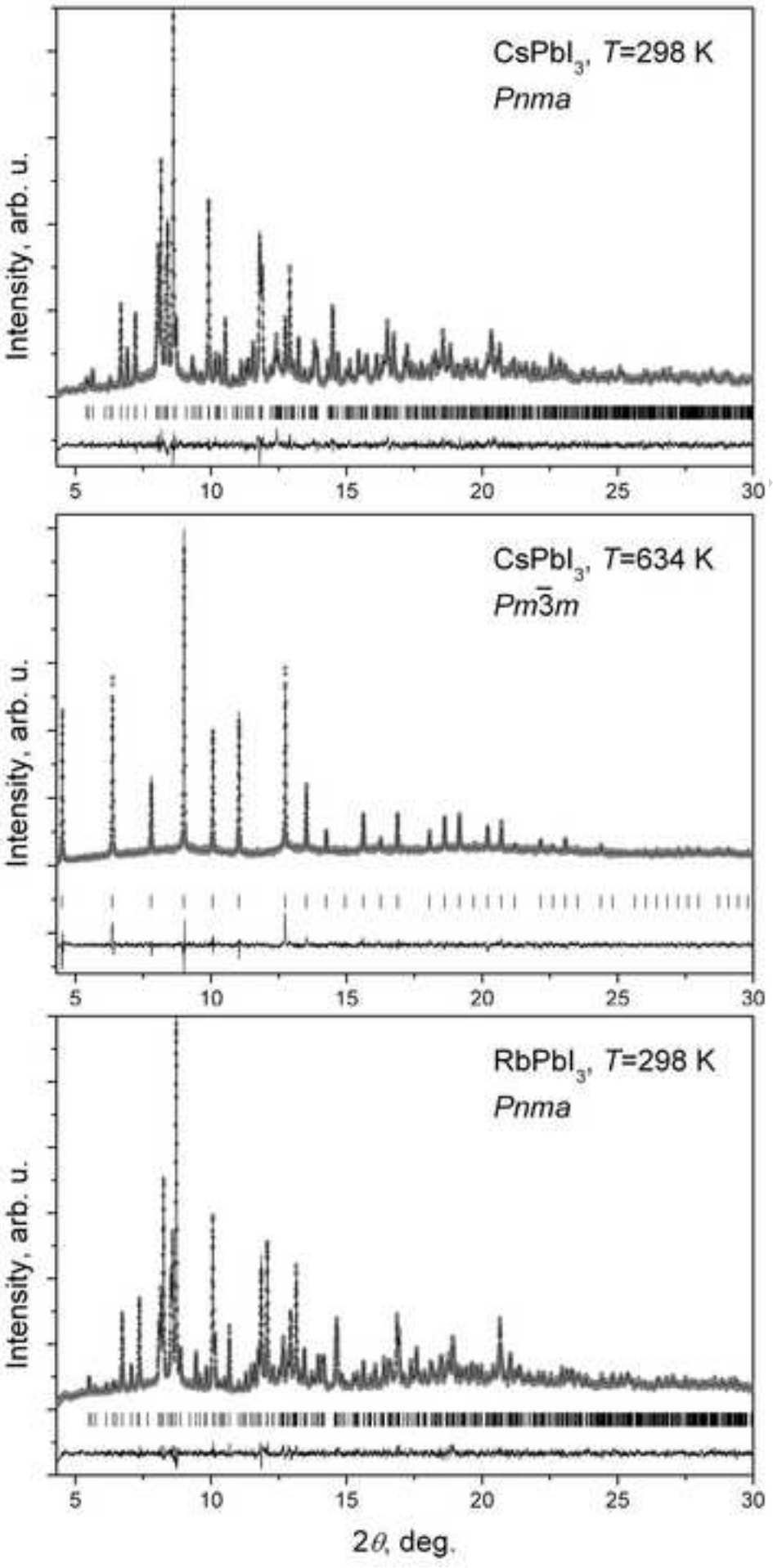

Figure2a

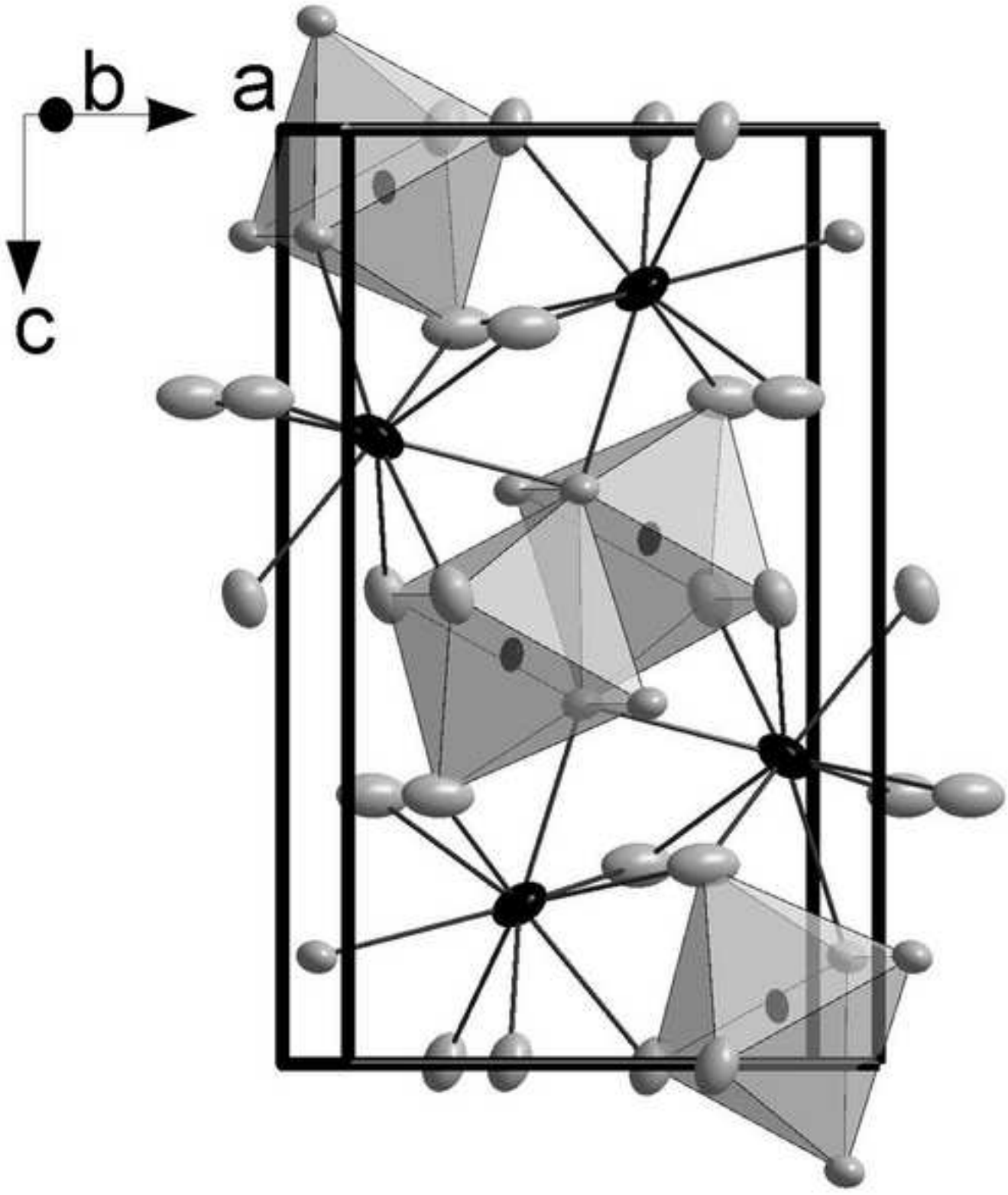

Figure2b

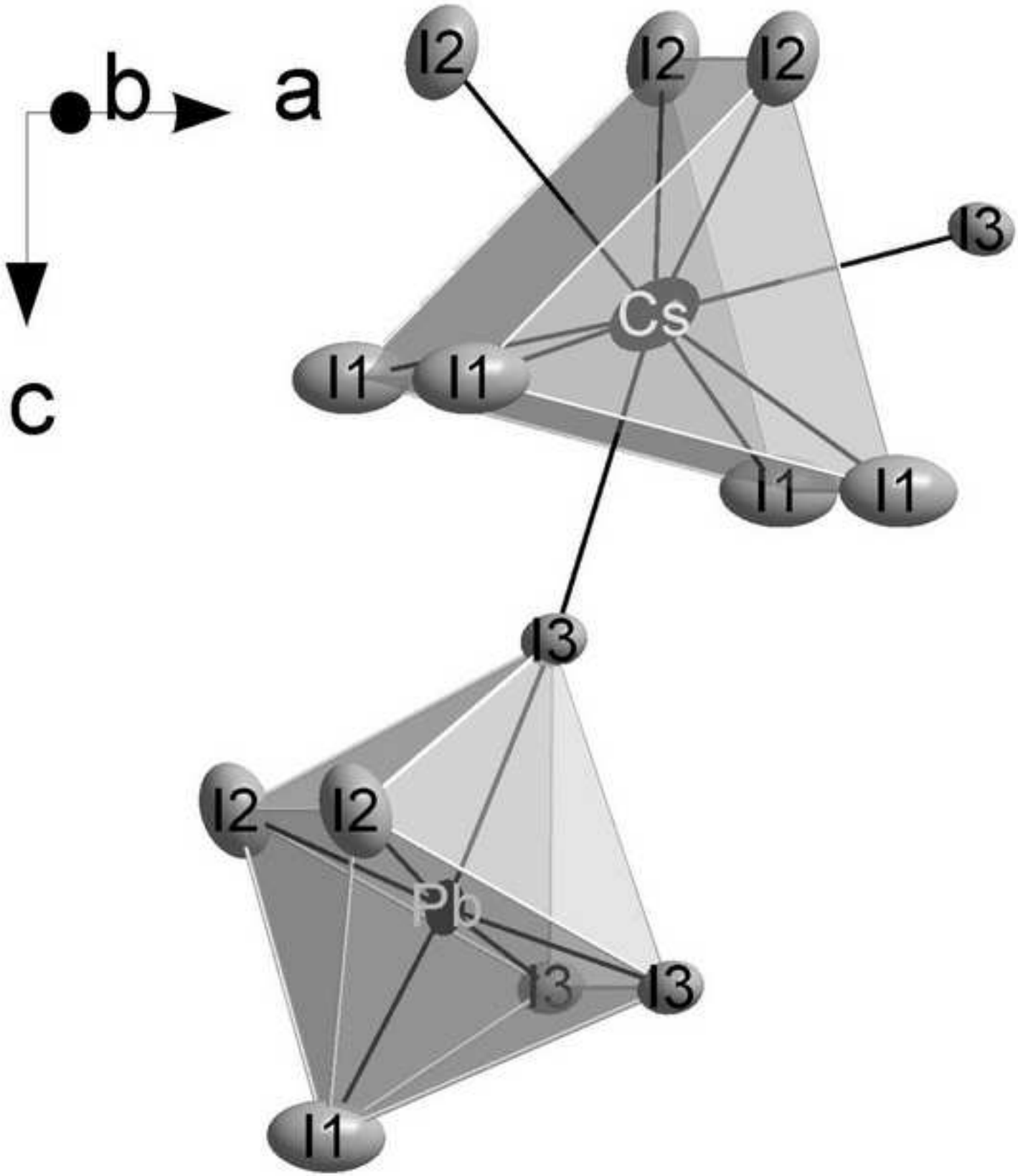

Figure2c

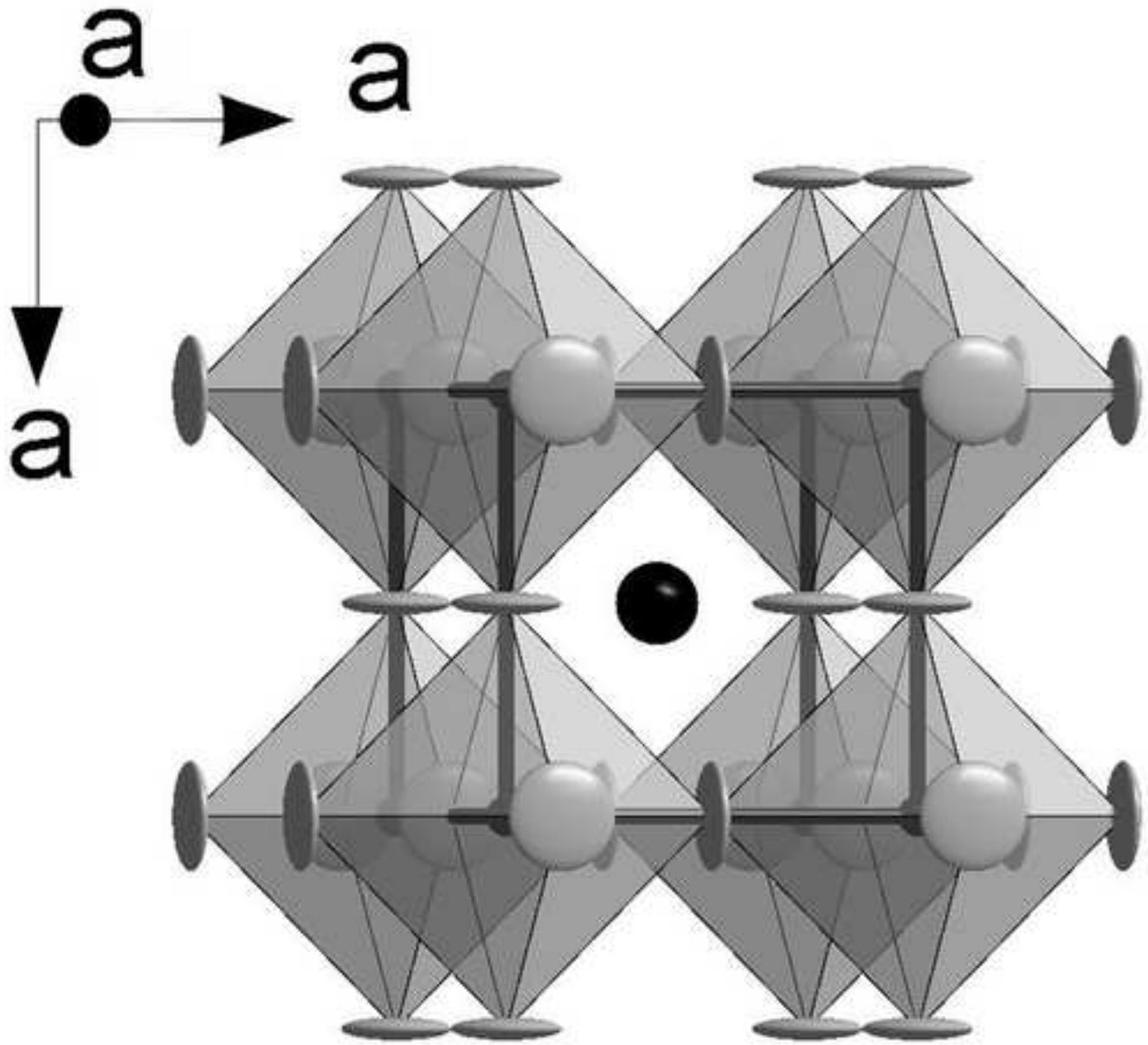

Figure3

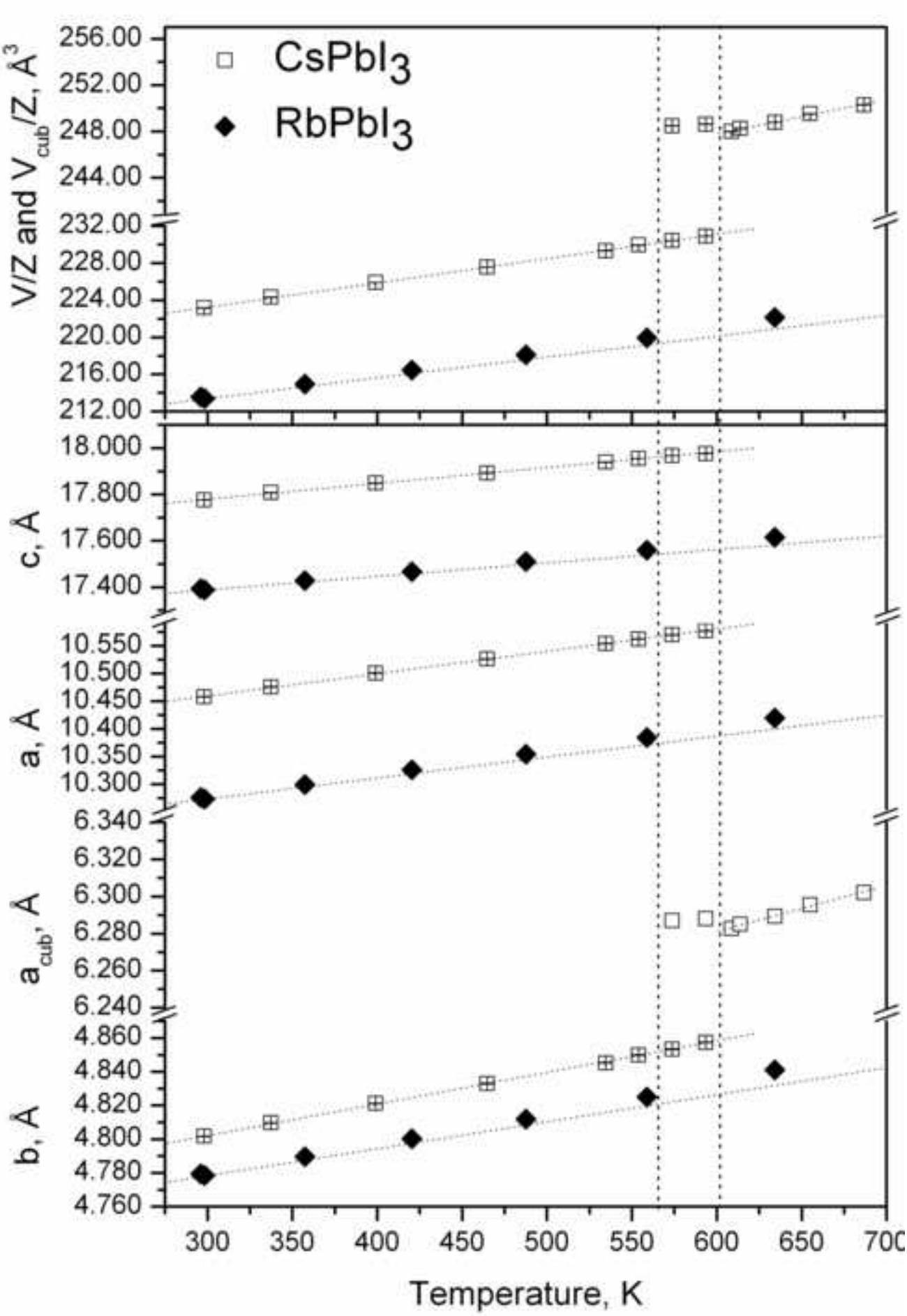

Figure4

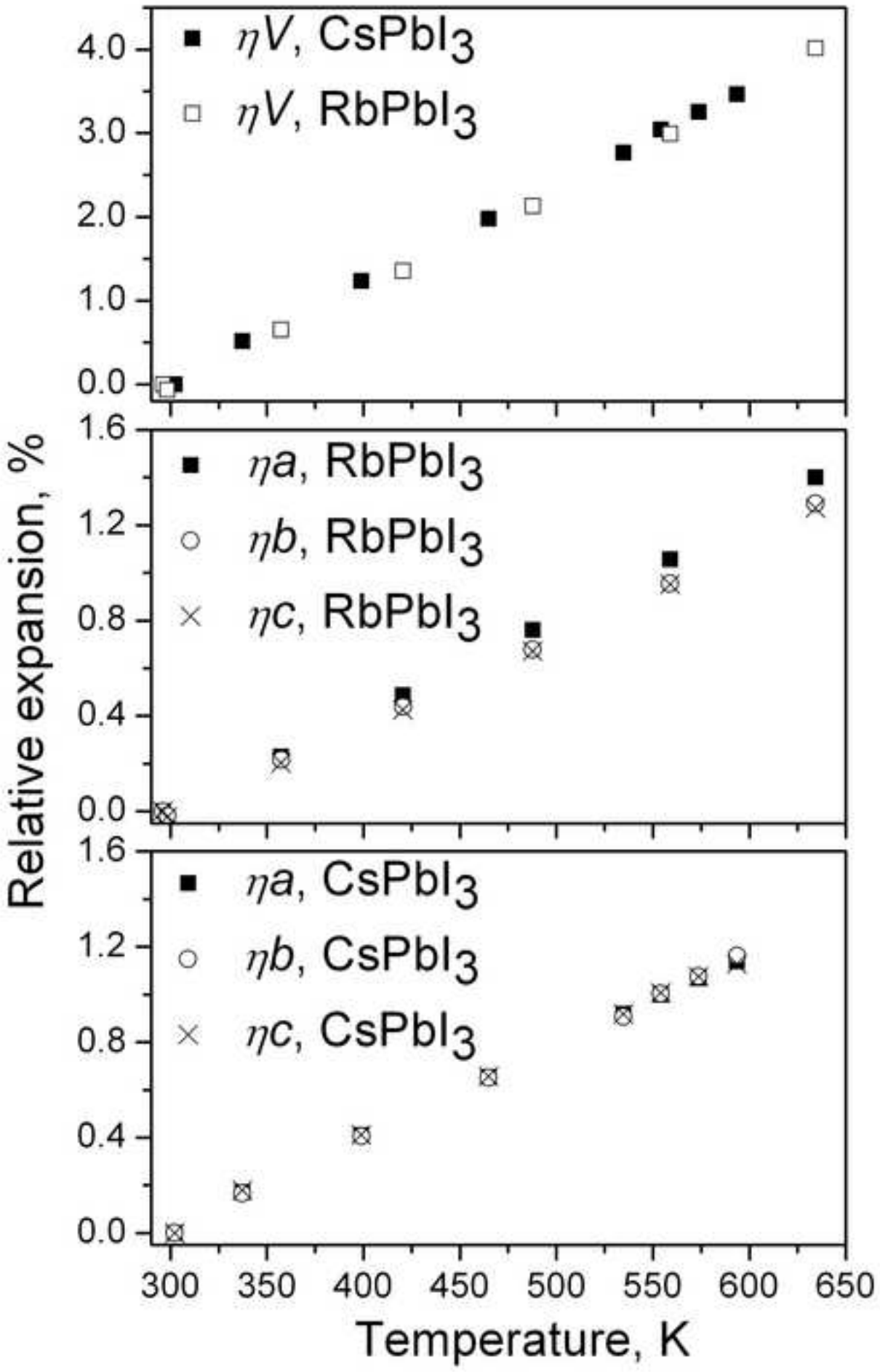

Figure5